

Trichoderma-Derived Pentapeptides from the Infected Nest Mycobiome of the Subterranean Termite *Coptotermes testaceus*

Markus Oberpaul,^[a] Stephan Brinkmann,^[a] Marius S. Spohn,^[a] Sanja Mihajlovic,^[a] Michael Marner,^[a] Maria A. Patras,^[a] Luigi Toti,^[b] Michael Kurz,^[b] Peter E. Hammann,^[b, d] Andreas Vilcinskas,^[a, c] Jens Glaeser,^{*[a, d]} and Till F. Schäberle^{*[a, c, e]}

Termites live in a dynamic environment where colony health is strongly influenced by surrounding microbes. However, little is known about the mycobiomes of lower termites and their nests, and how these change in response to disease. Here we compared the individual and nest mycobiomes of a healthy subterranean termite colony (*Coptotermes testaceus*) to one infected and ultimately eradicated by a fungal pathogen. We identified *Trichoderma* species in the materials of both nests, but they were also abundant in the infected termites. Meth-

anolic extracts of *Trichoderma* sp. FHG000531, isolated from the infected nest, were screened for secondary metabolites by UHPLC-HR MS/MS-guided molecular networking. We identified many bioactive compounds with potential roles in the eradication of the infected colony, as well as a cluster of six unknown peptides. The novel peptide FE011 was isolated and characterized by NMR spectroscopy. The function of this novel peptide family as well as the role of *Trichoderma* species in dying termite colonies therefore requires further investigation.

Introduction

Termites share a dynamic environment with many species of bacteria and fungi whose roles are not well understood. The mycobiomes of captive and free-living subterranean termites and their nest compartments have therefore been investigated to identify the dominant taxa.^[1–5] The genera *Debaryomyces*, *Candida*, *Exophiala*, GS23 (Umbelopsidomycetes), *Scytalidium*, *Talaromyces*, *Trichoderma* and *Xylaria* were found to be more

abundant in the nest material than the surrounding environment, and have the potential for both mutualistic and parasitic interactions.^[1–3] Mutualistic yeasts are present in the termite gut, where they facilitate the digestion of wood and support detoxification.^[6] Similarly, fungi present in termite nests, such as *Trichoderma* spp., may be mutualistic under most circumstances, but they may also be opportunists that can later become antagonistic, as shown for *Xylariales* spp.^[2,7–9] *Trichoderma* spp. produce a variety of secondary metabolites that may facilitate their interactions with termites.^[10] For example, they produce peptides such as trichodestruxins,^[11] trichovirins,^[12] trichorzins^[13] and peptaibols^[14] with antibiotic, antifungal and/or insecticidal activities.^[12,15–17] *Xylariales* spp. and *Trichoderma* spp. are ubiquitously distributed in natural environments, especially on rotting wood, but their relative abundance in the termite nest material and gut requires careful analysis.^[2]

Termites may recruit certain bacteria that synthesize natural products to maintain the nest biome and thus support colony fitness.^[4] We previously investigated the bacterial biomes of two captive subterranean termite nests (*Coptotermes testaceus*) over a period of 2 years. One nest was healthy, whereas the other was undergoing a microbiome shift caused by a fungal infection.^[18] Accordingly, we have now used this rare opportunity to also compare the mycobiomes of healthy and infected nests, as well as those of individual termites.

We isolated several fungal species from the infected samples including those representing the genera *Apiotrichum*, *Byssoscllamys*, *Exophiala*, *Galactomyces*, *Geotrichum*, *Penicillium* and *Trichoderma*. We focused on the secondary metabolites produced by *Trichoderma* spp. and analyzed them by UHPLC-HR MS/MS-guided molecular networking. Following automatic clustering of parent ions and subsequent manual data curation, a cluster containing unknown peptides was selected for

[a] M. Oberpaul, S. Brinkmann, Dr. M. S. Spohn, Dr. S. Mihajlovic, Dr. M. Marner, Dr. M. A. Patras, Prof. Dr. A. Vilcinskas, Dr. J. Glaeser, Prof. Dr. T. F. Schäberle
Branch for Bioresources


Fraunhofer Institute for Molecular Biology and Applied Ecology (IME)
Ohlebergsweg 12, 35392 Gießen (Germany)
E-mail: till.f.schaeberle@ime.fraunhofer.de


[b] Dr. L. Toti, Dr. M. Kurz, Prof. Dr. P. E. Hammann
Sanofi-Aventis Deutschland GmbH
Industriepark Höchst, 65926 Frankfurt am Main (Germany)

[c] Prof. Dr. A. Vilcinskas, Prof. Dr. T. F. Schäberle
Institute for Insect Biotechnology
Justus-Liebig-University Giessen
Heinrich-Buff-Ring 26–32, 35392 Giessen (Germany)

[d] Prof. Dr. P. E. Hammann, Dr. J. Glaeser
Evotec International GmbH
Marie-Curie-Straße 7, 37079 Göttingen (Germany)
E-mail: jens.glaeser@evotec.com

[e] Prof. Dr. T. F. Schäberle
Partner Site Giessen-Marburg-Langen
German Center for Infection Research (DZIF)
35392 Giessen (Germany)

 Supporting information for this article is available on the WWW under <https://doi.org/10.1002/cbic.202100698>

 © 2022 The Authors. ChemBioChem published by Wiley-VCH GmbH. This is an open access article under the terms of the Creative Commons Attribution Non-Commercial License, which permits use, distribution and reproduction in any medium, provided the original work is properly cited and is not used for commercial purposes.

detailed analysis. The most abundant derivative was isolated and structurally elucidated by NMR and MS/MS, and the structure of additional five derivatives was also tentatively proposed on the basis of their MS/MS fragmentation patterns.

Results and Discussion

The mycobiome differs between healthy and infected termite nests

A healthy and functional termite colony may require homeostasis of the bacterial and fungal biomes,^[19] although it is unclear why the nest mycobiome differs from the surrounding environment.^[2] The captive termite nests herein were reared for decades. We observed a fungal infection, which might have been introduced during the feeding routine of the colonies. It was speculated that the nest may have disrupted the microbiome balance. We therefore compared the infected colony to a healthy one to characterize the mycobiome. Hence, we recovered triplicate samples of material from various nest levels as well as termites from the healthy and infected colonies and characterized them by Illumina amplicon sequencing. We obtained 1,013,693 reads representing 446 operational taxonomic units (OTUs) and 146 phylogenetic groups from 27 samples (12 infected, 12 healthy, 3 fungal mat). Some groups were found in samples of both the healthy and infected environments, namely *Apiotrichum*, *Athrocladium*, *Candida*, *Colletotrichum*, GS23, *Hawksworthiomyces*, *Myrothecium*, *Shiraia*, *Vischniacozyma*, *Xylariales* and 'no hit' (Figure 1A). The genera *Debaryomyces*, *Stictis*, *Termitomyces* and *Wallemia* were solely connected to a healthy nest environment (Figure 1B). In contrast, the genera *Colacogloea*, *Exophiala*, *Malbranchea*, *Paecilomyces*, *Sugiyamaella*, *Scytalidium*, *Talaromyces* and *Trichoderma* were predominantly abundant in the infected nest material or termites.

The genera *Apiotrichum*, *Colletotrichum* and GS23 were highly abundant in healthy termite samples but absent in the termites suffering fungal infection (Figure 1B). *Paecilomyces*, *Sugiyamaella*, *Yamadazyma* and *Trichoderma* were prominently abundant in the infected termites and the material overgrown by fungus (Figure 1, S1). Similarity percentages breakdown (SIMPER) analysis was used to calculate the greatest statistical influence in the dataset.^[20] Although, this does not prove the contribution of particular genera towards termite health, it indicates possible influence factors. The analysis revealed a cumulative contribution of >80% by the phylogenetic groups *Apiotrichum* (20%), *Trichoderma* (11%), *Stictis* (8%), *Sugiyamaella* (8%), *Colletotrichum* (6%), *Debaryomyces* (6%), GS23 (6%), *Paecilomyces* (6%), *Candida* (4%), *Exophiala* (2%), *Talaromyces* (2%) and *Xylariales* (2%) (Table S1).

We also observed a spreading mycelial mat in the infected nest at a later stage (Figure S1). The abundance of *Xylariales* was low (3%) compared to all other phylogenetic groups, including *Apiotrichum* (26%), *Sugiyamaella* (26%), *Paecilomyces* (17%), GS23 (8%), *Scytalidium* (6%) and *Hawksworthiomyces* (4%) (Table S1; Figure 1A, Fungal mat), suggesting that *Xylar-*

iales alone is not responsible for the biome shift and eradication of the nest. However, representatives of *Xylariales* are often associated with fungus-growing termites^[21] and may act as specialized mutualists or opportunists given their presence in abandoned termite nests.^[2,22,23] They produce many natural products, including insecticides.^[24]

We also identified the genus *Exophiala* in infected termites and their nest (Figure 1A and B). This genus was reported as part of the microenvironment of leaf-cutting ants^[25] and other social insects.^[26] *Exophiala* spp. were found to produce an insecticidal natural product, causing larval mortality as well as deformities in emerging adults of *Spodoptera litura*.^[27]

Furthermore, *Paecilomyces* spp. were abundant in all samples, but particularly in the infected specimens (Figure 1). The entomopathogenic genus *Isaria* (formerly *Paecilomyces*) was reviewed and patented as a biocontrol agent against plant pathogens, nematodes, and insects,^[28] especially to control Formosan subterranean termites.^[29] *Paecilomyces* spp. produce multiple bioactive substances including insecticides and mycotoxins.^[28,30] *Trichoderma* spp. were the most abundant in the infected termite individuals (Figure 1A). *Trichoderma* spp. are abundant in habitats linked to termites that feed on decayed wood, but it is unclear whether they are beneficial or detrimental.^[2,3,8,31] They are ubiquitous saprophytes and endophytes that produce numerous secondary metabolites,^[32] including bioactive peptaibols, alkaloids, polyketides and non-ribosomal peptides (NRPs)^[16,17] with antibacterial, cytotoxic, antifungal, antiviral and anti-inflammatory properties.^[10,33] *Trichoderma virens* and others have been evaluated as biocontrol agents against subterranean termites.^[34] The phytotoxic fungal steroid viridiol and the peptaibol trichokonin VI are produced by several *Trichoderma* species.^[10,16,35] Trichokonin VI, a Ca²⁺ channel antagonist,^[36] suppresses plant cell division and proliferation,^[37] whereas viridiol kills plant cells and bacteria.^[38]

In summary, these data suggest that *Exophiala*, *Paecilomyces*, *Trichoderma* and *Xylariales* are involved in the changing health of the termite colony. However, the abundance of individual taxa cannot explain the interactions between biomes and their impact on colony health. Thus, we herein focused on the screening of secondary metabolites produced by *Trichoderma* spp. using a molecular networking approach.

Structural analysis of the novel pentapeptide FE011

We used potato dextrose agar (5367) to culture fungi from the infected samples. Propagation and subsequent partial 18S rRNA gene sequencing (only NS1) indicated the presence of axenic cultures belonging to the genera *Apiotrichum*, *Byssoschlamys*, *Exophiala*, *Galactomyces*, *Geotrichum*, *Penicillium* and *Trichoderma*. The complete 18S rRNA sequence (NS1 and FR1) alignment of strain FHG000531 (Figure S1), which was isolated from infected nest material, was 99.9% identical to *Trichoderma longibrachiatum* H9^T, *T. harzianum* Iy9-12^T and *T. reseei* Qm6a^T.^[39] To determine the metabolic profile of the new strain, we grew it in five different media for 4 and 7 days. Subsequently, methanolic extracts were prepared for analysis by mass

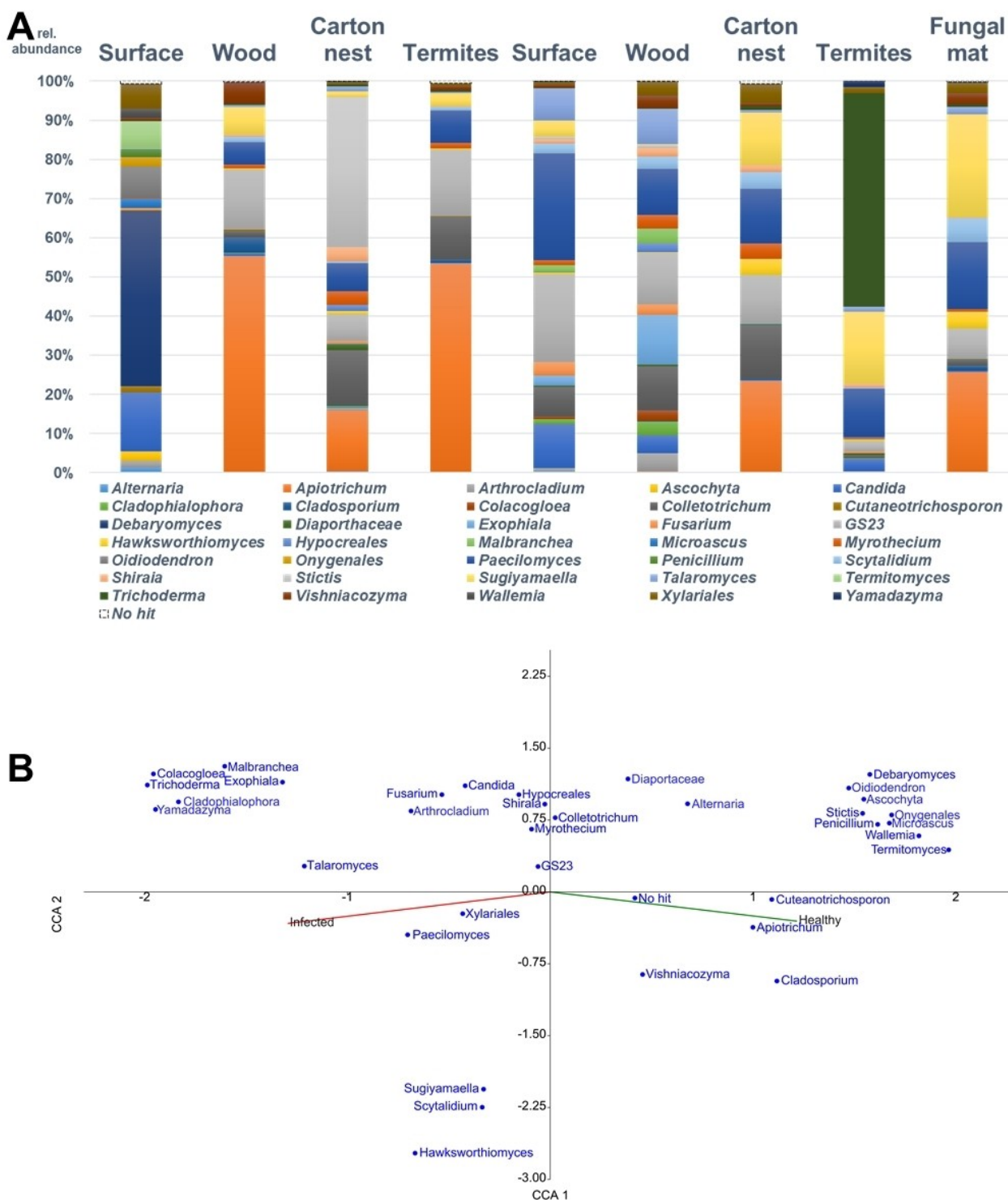


Figure 1. Phylogenetic analysis of *Coptotermes testaceus* termite nests. (A) Comparative abundance of fungal phylogenetic groups at the genus level in healthy and infected captive *C. testaceus* termite nests and specimens, and their correlation with colony health. Three replicates of each sample were used to calculate the mean percentage. (B) Canonical correspondence analysis (CCA) triplot of all Illumina amplicon sequencing data with the greatest influence on the dataset (> 80%). The numbers of the axes (no dimension) represent the distances between the samples. Similar objects are located near to each other and dissimilar objects are farther apart from each other. Inclusion of two environmental factors 'healthy' and 'infected' resulted in a triplot, which displays the relationship of the fungal genera to colony health status.^[20] Three replicates were used to determine the mean abundance of fungal ITS2 gene sequence affiliations. All data (healthy and infected nests and specimens) were used for the calculation, revealing that certain phylogenetic groups associate more with infected nest material or specimens than healthy ones.

spectrometry (MS) including molecular networking. By screening Antibase^[40] and our in-house database (at the time containing ~1700 structurally characterized metabolites), we annotated 24 clusters (≥ 3 nodes) by using *in silico* MS/MS fragmentation comparison (Table S2). This indicated the potential of strain FHG00531 to produce bioactive secondary metabolites. For example, known parent masses were affiliated to destruxin A (m/z 578.354 $[M+H]^+$), viridiol (m/z 355.117 $[M+H]^+$), trichokonin VI (m/z 647.04 $[M+3H]^{3+}$), and desferri-ferricrocin (m/z 718.337 $[M+H]^+$), which are part of our in-house database (Figure 2). Destruxins are hexadepsipeptides with activity against several bacteria, fungi^[41] and insects, including *S. litura* larvae.^[42] These compounds open Ca^{2+} channels in insects, causing tetanic contraction and ultimately death.^[43] Furthermore, we identified an unknown cluster of metabolites containing an abundant ion (m/z 703.485 $[M+H]^+$)

with the predicted molecular formula $C_{36}H_{63}N_8O_6$ and five derivatives thereof (Figure 2 and Figure 3).

MS/MS fragmentation data indicated a set of related peptides (Figures S3–S8). *Trichoderma* spp. produce peptides with properties suitable for biotechnological and agricultural applications.^[10,14] We therefore selected this cluster of metabolites for further analysis.

MS/MS fragmentation analysis of the unknown peptide 1 (FE011) (depicted in Table 1) revealed a C-terminal Arg (aa5), one Leu/Ile (aa3), one Phe (aa2), and a neutral loss unit of 127.0999 Da (aa4) with the predicted molecular formula $C_7H_{12}N_1O_1$ (suggesting methylated Leu/Ile) and an N-terminal unit with the formula $C_8H_{14}N_1O_1$ (Figure S3). The target ion (m/z 703.4870 $[M+H]^+$) was isolated for analysis by NMR spectroscopy due to its prominence in the methanolic extract of potato dextrose broth (PDB). The structure was determined by

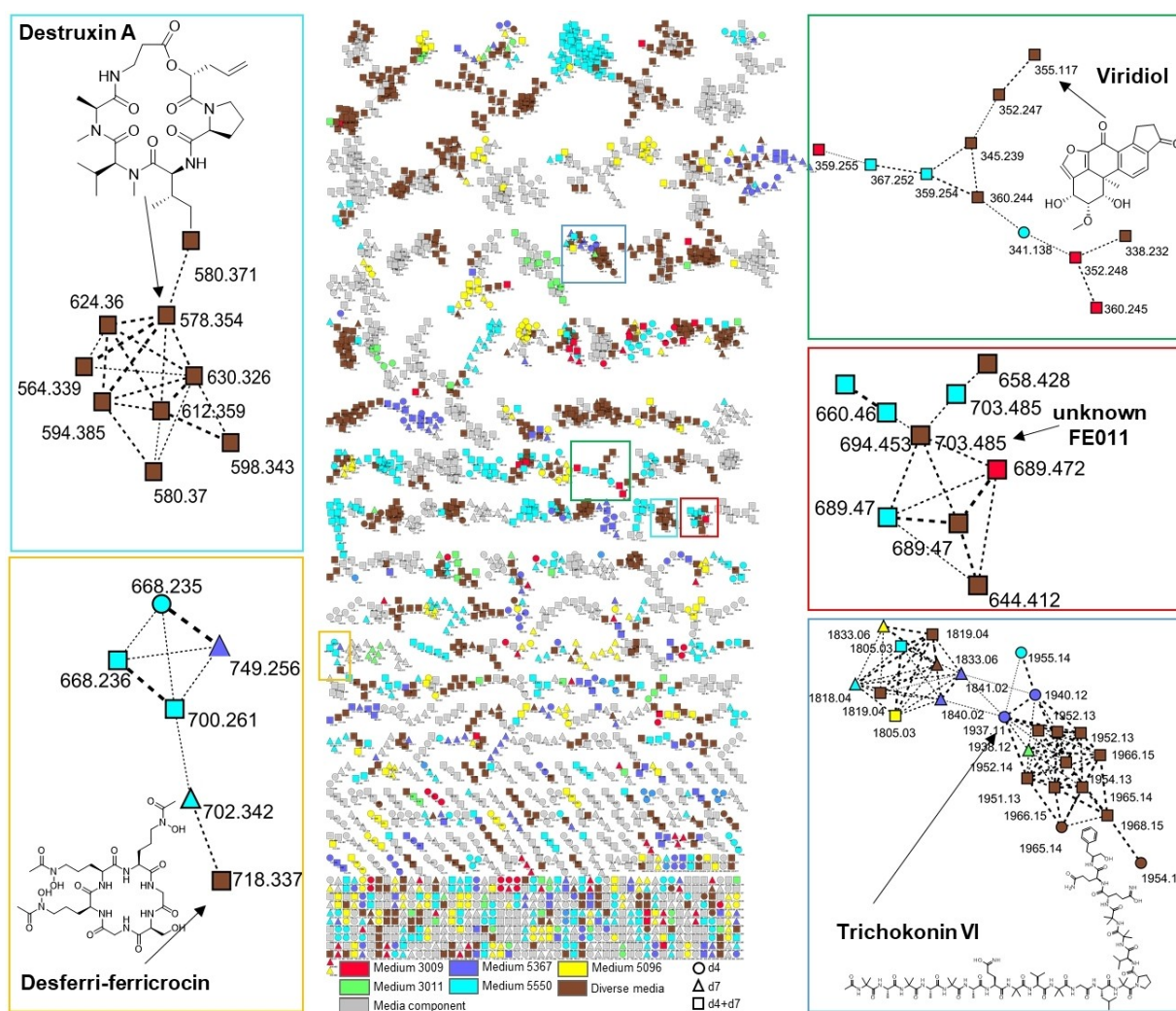


Figure 2. MS/MS molecular networking of all methanolic extracts derived from *Trichoderma* strain FHG00531 grown in five different media. Different known clusters are highlighted in color, focusing on the cluster representing peptide FE011 and its derivatives. Twenty-four clusters were annotated following *in silico* generated fragment spectra (Table S2). Each dot represents a single parent ion. Colors represent the culture medium associated with the parent ion: red = medium 3009, green = medium 3011, yellow = medium 5096, violet = medium 5367, blue = medium 5550, brown = parent ion was detected in more than one media used herein and is not a medium component. If parent ions were also detected in any of the five used media, dots were colored gray. Shapes represent the day of detection: circle = exclusively produced at day 4, triangle = exclusively produced at day 7. If produced on both days 4 and 7, dots were displayed as square. Cytoscape v3.8.2 was used to visualize the data.^[54–58]

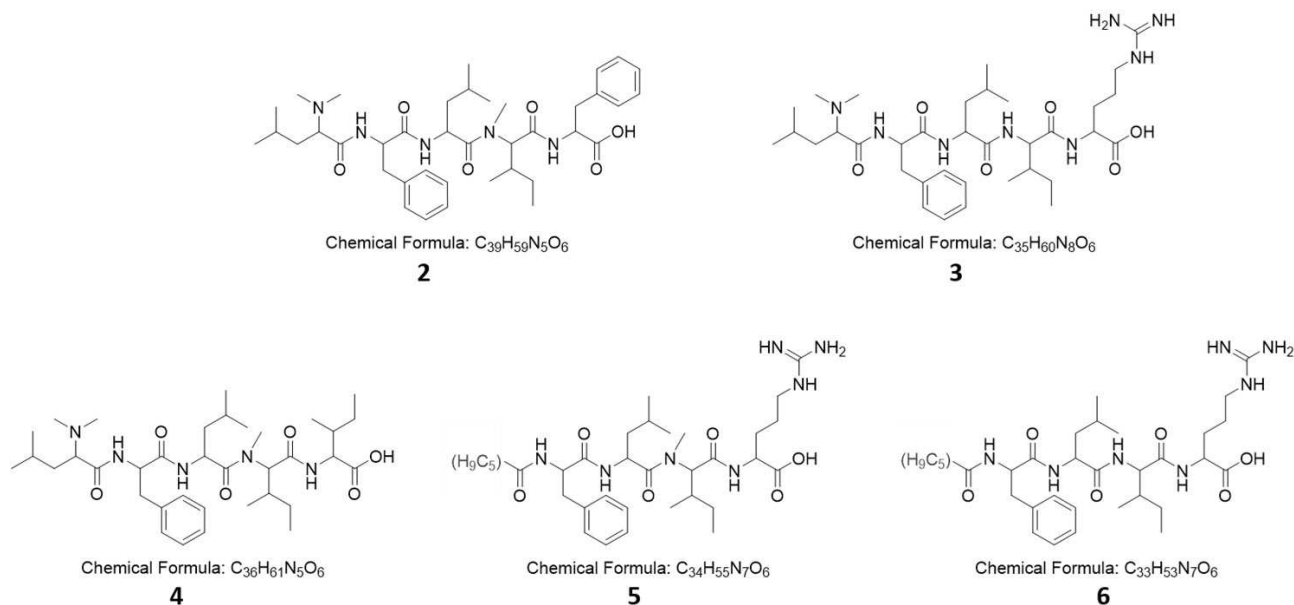


Figure 3. Tentative structures of the FE011 derivatives, inferred from the MS/MS signatures. For all compounds, structures of Leu and Ile were conventionally chosen to depict aa3 and aa4, respectively, by analogy with the elucidated structure of FE011. For compounds 2–4, *N,N*-dimethyl-Leu was conventionally chosen to depict aa1, by analogy with the elucidated structure of FE011. For compounds 5 and 6, identity of the C6:1 fatty acid remains open.

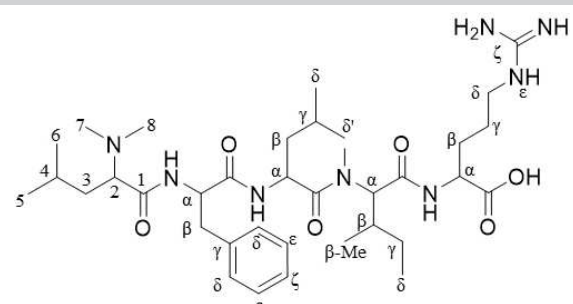
comprehensive NMR analysis, comprising 1H , ^{13}C , ROESY, TOCSY and HSQC spectra (Figures S9–S13). This revealed the presence of the three natural amino acids Phe, Leu and Arg (Figures S9–S13). In addition, we identified spin systems of a second Leu and an Ile side chain that did not include an amide proton. For the Ile residue, the amide proton was replaced with a methyl group, as indicated by correlation between the $C\alpha$ of the Ile and *N*-methyl protons (2.93 parts per million [ppm]) in the HMBC spectrum. Likewise, the $C\alpha$ of the second Leu revealed a coupling to a singlet at 1.91 ppm, corresponding to six protons and thus indicating the structure of an *N,N*-dimethyl-Leu residue. The sequential assignment was based predominantly on correlations in the ROESY spectrum, in particular three $NH_i + 1/H\alpha_i$ correlations (Arg-NH/*N*-methyl-Ile- $H\alpha$, Leu-NH/Phe- $H\alpha$ and Phe-NH/*N,N*-dimethyl-Leu- $H\alpha$) and a close correlation between the *N*-methyl group of *N*-methyl-Ile and the $H\alpha$ proton of Leu (Figure S13). These correlations led to the sequence *N,N*-dimethyl-Leu-Phe-Leu-*N*-methyl-Ile-Arg (Table 1, Figure S13). The incorporation of *N,N*-dimethyl-Leu introduces an unusual adduct that is poorly described.^[44] The stereochemistry was solely elucidated for the proteinogenic amino acids of **1**, which are L-Phe as aa2, L-Leu as aa3 and L-Arg as aa5 (Figure S14).

Identification of five additional FE011 derivatives

For the remaining five compounds in the cluster, manual analysis of the MS/MS fragmentation patterns confirmed their structural similarity to FE011 (Figures S3–S8). Ion 689.4717 [M + H]⁺ was found in at least two isomeric forms, that were only present in medium 3009 and 5550 on both days (Figure 2). Pentapeptide **2** differs from FE011 at the C-terminus, where Arg

is replaced with Phe (Figure 3). Pentapeptide **3** is an *N*-demethylated analog of **1**, lacking the methyl-Ile at position 4. Pentapeptide **4** differs from **3** at the C-terminus, where Arg is replaced with Leu/Ile (MS cannot distinguish between isobaric units, so the C-terminal amino acid remains unclear). Compound **5** is a lipo-tetrapeptide in which the *N,N*-dimethyl-Leu at position 1 in FE011 is replaced with a C(6:1) fatty acid, inferred from the neutral loss of 96.0575 Da. Compound **6** is the *N*-demethylated analog of **5** (Figure 3). Interestingly, the differences between the derivatives were not confined to alternative methylation, but also included the replacement of terminal amino acids. The methylation of amino acids by methyltransferases can take place before or after peptide synthesis.^[45] Backbone *N*-methylation of (cyclic) peptides alters the conformation, can dramatically improve receptor subtype selectivity and synchronize oral bioavailability, and is therefore added to improve pharmacokinetics in medicinal chemistry.^[46,47] *N*-Methylation of exposed amino groups enhances passive permeability,^[48] increases stability and thus confers a longer half-life *in vivo*.^[46]

Given the antimicrobial effects of several *Trichoderma* metabolites,^[38,49] we tested purified compound **1** against *Escherichia coli* ATCC 35218, *Staphylococcus aureus* ATCC 25923, and *Mycobacterium smegmatis* ATCC 607 for antibacterial activity, against *Aspergillus flavus* ATCC 91 for antifungal activity, against *Brassica rapa* subsp. *rapa* for phytotoxic activity, and against *C. elegans* for activity against invertebrates. However, no bioactivity was observed against a microbial and fungal panel (>64 μ g/mL), against *B. rapa* subsp. *rapa* at concentrations up to 10 μ M, against *C. elegans* (>64 μ g/mL) and MDCK II cells (Table S3, Figure S15). Therefore, the biological role of **1**

Table 1. The ^1H (600 Mz) and ^{13}C (150 MHz) NMR data for FE011 in DMSO- d_6 at 303 K.


Chemical Formula: $\text{C}_{36}\text{H}_{62}\text{N}_8\text{O}_6$

1

	δ ^1H [ppm]	δ ^{13}C [ppm]
<i>N,N</i>-di-Me-Leu		
1	–	170.86, C
2	2.82, t (7.2)	65.52, CH
3	1.26, m	~38.1 (b), CH_2
4	1.35, m	24.42, CH
5	0.81, m	22.32, CH_3
6	0.76, m	22.97, CH_3
7,8	1.91, s	41.37, CH_3
Phe		
NH	7.86, d (8.4)	–
A	4.63, m	~53.0 (b), CH
B	2.97/2.73	~37.4 (b), CH_2
γ	–	137.7 (b), C
δ	7.25, m	129.15, CH
ϵ	7.22, m	127.82, CH
ζ	7.15, m	~126.1 (b), CH
C'	–	171.01, C
Leu		
NH	8.27, d (8.3)	–
A	4.78, m	~46.8 (b), CH
B	1.46/1.38, m	~40.4 (b), CH_2
γ	1.59, m	24.11, CH
δ	0.87, m	23.00, CH_3
δ'	0.86, m	21.67, CH_3
C'	–	172.16, C
NMe-Ile		
Nme	2.93	29.96
α	4.65	~59.8 (b)
β	1.95	~31.0 (b)
β -Me	0.83	15.40
γ	1.27/0.89	23.92
δ	0.78	10.28
C'	–	n.a.
Arg		
NH	7.20, b	–
α	3.85, b	~52.8 (b), CH
β	1.59, m	~28.9 (b), CH_2
γ	1.40, m	~24.8 (b), CH_2
δ	3.04, b	~40.3 (b), CH_2
ϵ	n.a.	–
ζ	–	n.a.
C'	–	~173.8 (b), C

n.a. = not available.

remains unclear and should be investigated in more detailed studies using a wider range of assays.

Conclusion

The novel pentapeptide FE011 (**1**) was isolated from *Trichoderma* sp. FHG000531, which was enriched in an infected termite nest. Phytotoxic, antibacterial, antifungal, and insecticidal metabolites were dereplicated by molecular networking. However, FE011 showed no bioactivity in our panel of tests, so its function remains unclear, as does the role of *Trichoderma* spp. in wood-feeding subterranean termites.^[2,4,7,14,31] Besides *Trichoderma*, other abundant fungi in the infected nest were isolated including *Exophiala*, *Paecilomyces*, *Trichoderma*, *Penicillium* and *Xylariales*. From these genera the production of insecticidal secondary metabolites is reported, and therefore they might have been involved in the changing health status of the termite colony. Thus, further experiments on the mycobiome of the nest and isolates thereof are required to gain insight into the inter-kingdom relationships and interactions within the termite biomes. This could shed light on the ecology of termites and their related fungi, offering strategies for termite pest control involving the introduction of fungi that affect termite fitness.

Experimental Section

Rearing of captive termites and sampling procedure: The captive colonies of *C. testaceus* (Ct) were identified based on their morphological characters.^[50] They originate from British Honduras and their rearing started in 1972 at the Federal Institute for Materials Research and Testing (BAM) in Berlin, in separate metal tanks with a volume of ~2 m³. Colonies were reared at 29 ± 2 °C and 75 ± 5% relative humidity, and were fed on pine wood every 3 months. We collected three samples from each nest level (*wood* [W], *surface* [S] and *carton nest* [C]) as well as three termite soldiers from a healthy (*h*) nest (Figure S1A) and an infected (*i*) nest (Figure S1B). For all termite samples, filter carton paper traps were placed in the nests to separate the termite soldiers from the nest material (Figure S16) using soft tweezers. The termite specimens were then collected in 50-mL tubes and directly frozen (*termites* [T]). We also collected three replicates of a piece of material overgrown by a fungal mat at a later stage of infection (*fungi* [F]) (Figure S1C,D). All samples were frozen and stored at –50 °C for processing or at 4 °C for cultivation.

Illumina amplicon sequencing: Nucleic acids were extracted from the samples using the NucleoSpin soil DNA purification kit (Macherey Nagel, Düren, Germany). To increase the yield, ~500 mg of nest material or 20 termites were transferred to the NucleoSpin bead tubes before adding 700 μL of lysis buffer SL2. The tubes were vortexed horizontally for 15 min at 40 Hz using a Top Mix 11118 (Thermo Fisher Scientific, Schwerte, Germany) and centrifuged at 12,000 × *g* for 2 min. Subsequent extraction steps were carried out according to the manufacturer's recommendations. Finally, the yield and purity of the DNA was checked using a NanoDrop ND-1000 UV/Vis spectrophotometer (Thermo Fisher Scientific) and adjusted to 5 ng/mL. Illumina amplicon sequencing on a Miseq V₃ device (Illumina, San Diego, CA, USA) was carried out by LGC Genomics (Berlin, Germany) using degenerate primer pair ITS7F (5'-GTG ART CAT CGA ATC TTT G –3') and ITS4R (5'-TCC TCC GCT TAT TGA TAT GC-3'). Demultiplexing of libraries for each sequencing lane was achieved using Illumina bcl2fastq v2.17.1.14 (<https://support.illumina.com/downloads/bcl2fastqconversion-software-v2-19.html>). Reads with missing barcodes, one-sided barcodes or conflicting barcode pairs were discarded. The sequence frag-

ments were converted to forward-reverse primer orientation after removing the primer sequences and combined using BBMerge v34.48 (<http://jgi.doe.gov/data-and-tools/bbtools>). To identify OTUs, the resulting file was processed using the PIPITS pipeline.^[51] The automatic classification was manually curated and completed by affiliation to the most similar genus using the pairwise alignment tool from Mycobank.^[52] Non-identifiable sequences (0.2%) were classified as 'no hit' in the database. Three replicates of each sample were combined for further analysis to reduce the influence of outliers. The Illumina amplicon sequencing data supporting the findings of this study are openly available under the BioProject PRJNA788263 (<https://www.ncbi.nlm.nih.gov/bioproject/PRJNA788263>).

Statistical analysis: Statistical analysis was carried out using PAST v4.03.^[53] Canonical correspondence analysis (CCA) was used to compare the mycobiomes of the healthy and infected nests, complemented by an analysis of similarities (ANOSIM) and an analysis of the similarity percentage (SIMPER) to identify data with the greatest statistical effect in the whole data set.^[20]

Media preparation: Difco PDB (VWR, Radnor, PA, USA) was prepared according to the manufacturer's protocol, with an additional 0.20 g/L yeast extract to give medium 5367. Basal salt medium (BSM) was prepared as described before.^[54] This was supplemented with 10 g/L xylan and 10 g/L xylose, and brought to pH 7 with NaOH to prepare medium 3011. BSM was supplemented with 10 g *N*-acetylglucosamine and 10 g chitin instead of xylan and xylose to prepare medium 3009. Rice medium (5550) was prepared by weighing 40 g of rice grains into a 300-mL Erlenmeyer flask and adding 40 mL of fresh medium 3011 before autoclaving. Tomato/cornsteep medium (5158) was prepared by mixing 5 g cornsteep liquid, 40 g tomato paste, and 10 g ground oatmeal with 1 L MilliQ water, then adding 1 mL of trace element solution (1.0 g/L $\text{FeSO}_4 \times 7\text{H}_2\text{O}$, 1.0 g/L $\text{MnSO}_4 \times 1\text{H}_2\text{O}$, 0.05 g/L $\text{CuCl}_2 \times 2\text{H}_2\text{O}$, 0.1 g/L $\text{CaCl}_2 \times 2\text{H}_2\text{O}$, 0.01 g/L H_3BO_3 , 0.02 g/L $(\text{NH}_4)_6\text{Mo}_7\text{O}_{24} \times 4\text{H}_2\text{O}$ and 0.2 g/L $\text{ZnSO}_4 \times 7\text{H}_2\text{O}$) and adjusting the pH to 6.8 before autoclaving.

Cultivation and propagation of isolated fungi: Material from the infected termite nest (500 mg) was weighed into 50-mL tubes and mixed with 10 mL PBS. The slurry was homogenized for 5 s at 225 Hz using an S25 KD 18 G dispersal tool connected to an Ultra-Thurax T25 basic (IKA Werke, Staufen im Breisgau, Germany). The suspension was distributed onto PDB agar (5367) plates in three 10-fold dilutions starting from 10^{-3} . The plates were incubated at 25 °C. Growing colonies were transferred daily to fresh 5367 until axenic cultures were obtained. Isolated pure colonies were stored in 80% glycerol (v/v) in liquid nitrogen.

Phylogenetic classification of strains by 18S rRNA gene sequencing: Fungal culture broth (500 μL) was collected in 1.5-mL tubes and the cells were pelleted by centrifugation (12,000 $\times g$, 30 s). We added 700 μL lysis buffer SL2 from the NucleoSpin soil DNA kit, two 3-mm tungsten carbide beads (69997; Qiagen, Hilden, Germany) and two 12.3-mm zirconia beads (N036; Carl Roth, Karlsruhe, Germany), then disrupted the cells in a TissueLyser II (Qiagen) twice at 30 Hz for 30 s. DNA was extracted using the NucleoSpin soil DNA kit, starting with the precipitation step of the manufacturer's protocol. The purified DNA was used as the template for 18S rRNA gene amplification with primer pair NS1 (5'-GTA GTC ATA TGC TTG TCT C-3') and FR1 (5'-AIC CAT TCA ATC GGT AIT-3') as previously described.^[55] Ambiguities were manually curated, the forward and reverse strands were aligned, and the sequences were affiliated to the most similar genus using the pairwise alignment tool from Mycobank.^[52] Data supporting the findings of this study are available under the BioProject PRJNA788263 (<https://www.ncbi.nlm.nih.gov/bioproject/PRJNA788263>).

Fermentation of fungal strains: Glycerol stocks were inoculated into medium 5367 and cultivated as above for 4 days, transferred to 5367 agar plates for 4 days, then inoculated into fresh medium 5367 and cultivated for another 4 days. From this pre-culture, fresh batches of medium 3009, 3011, 5096, 5367 and 5550 were inoculated (5% v/v) in Erlenmeyer flasks and incubated at 25 °C, shaking at 180 rpm with a 5-cm deflection. After 4 or 7 days of fermentation, the broth was freeze-dried and 50-fold methanolic extracts were prepared.

Isolation of the unknown peptide FE011: *Trichoderma* strain FHG000531 was inoculated 10 \times from the same agar plate into 30 mL PDB in 100-mL Erlenmeyer flasks at 25 °C, shaking at 180 rpm with 5 cm deflection for 4 days. The culture broth was then combined to inoculate 2-L Erlenmeyer flasks (5% v/v) under the same conditions. After 4 or 7 days, cell pellets were separated from the culture broth, and both components were frozen at -50 °C and subsequently lyophilized. The dried cell pellets were extracted with a 1:40 mixture of water and dichloromethane, and the water phase was evaporated under vacuum. The resulting dry extract was extracted three times with 3 L methanol, and all three organic phases were combined and dried. The dried cell-free supernatant was also extracted four times with 2 L methanol and dried as above. Both extracts were reconstituted in water containing 10% methanol, combined, and sequentially fractionated on an XAD16 N column (~1 L bed volume). Following stepwise elution in ~2 L 20%, 40%, 60% and 80% methanol in water, the fractions were identified by UHPLC-UHR-MS using a maXisII device (Bruker Daltonics, Bremen, Germany). Fractions containing FE011 were combined *in vacuo* and adjusted to 200 mg/mL using methanol for preparative HPLC on a Synergi 4u Fusion-RP column (80 Å, 250 \times 21.2 mm) over 16.5 min in a linear gradient of 5–50% acetonitrile containing 0.1% formic acid. Target fractions were dried *in vacuo* and redissolved in methanol to a concentration of 30 mg/mL before elution by semi-preparative HPLC on a Nucleodur C18 Gravity-SB column (3 μm , 150 \times 2 mm) over 25 min in a linear gradient of 5–95% acetonitrile. Final purification was achieved by UHPLC on an Acquity UPLC BEH C18 column (130 Å, 1.7 μm , 100 \times 2.1 mm) coupled to a custom-made fraction collector (Zinsser Analytics, Eschborn, Germany) over 10 min with a linear gradient of 5–60% acetonitrile.

Mass spectrometry: We used a 1290 UHPLC system (Agilent Technologies, Santa Clara, CA, USA) equipped with DAD, ELSD and maXis II (Bruker Daltonics). Samples were separated in a gradient of solvent A (0.1% formic acid in water) and solvent B (0.1% formic acid in acetonitrile) at a flow rate of 600 $\mu\text{L}/\text{min}$. The following program was used: 0 min, 95% A; 0.30 min, 95% A; 18.00 min, 4.75% A; 18.10 min, 0% A; 22.50 min, 0% A; 22.60 min, 95% A; 25.00 min, 95% A. We used an Acquity UPLC BEH C18 column (1.7 μm , 2.1 \times 100 mm) with an Acquity UPLC BEH C18 VanGuard Pre-Column (1.7 μm , 2.1 \times 5 mm) at 45 °C, with an injection volume of 2 or 5 μL . All data were analyzed with the Bruker Data Analysis 4.0 software package (Bruker Daltonics).

Molecular networking and automated UHPLC-HR MS/MS-guided dereplication *in silico*: Dereplications of known and unknown metabolites from UHPLC-HR MS/MS data were achieved by comparing chromatograms derived from all extracts using molecular networking (five different media, sampled at d4 and d7 including controls) as described before.^[54] In brief, by using MSConvert (ProteoWizard package^[56]) raw data were converted to plain text files (.mgf), which contained MS/MS peak lists, wherein each parent ion is signified by a list of fragment mass/intensity value pairs (peak picking: vendor MS level = 1–2; threshold: absolute intensity, 1000, most intense). Molecular networking was performed by applying established

protocols using a cosine similarity cutoff of 0.7.^[57] In addition, ions need a minimum of six shared fragments (tolerance 0.05 Da) with at least one partner ion to be depicted in the final molecular networking. *In silico*, the retention time and fragmented compounds^[58] were compared with our in-house reference database containing > 1700 characterized metabolites at the time of data evaluation.^[54] We also used the freely accessible AntiBase^[40] (AB) 2017 and the Dictionary of Natural Products (<http://dnp.chemnetbase.com/faces/chemical/ChemicalSearch.xhtml>; accessed Nov 16, 2020) for molecular formula searches as previously described,^[59] which implies different degrees of confidence for the obtained annotations.^[60] Cytoscape v3.8.2 was used to visualize the data as a network comprising nodes and edges, wherein each node represents a parent ion and its color reflects the sample (see caption Figure 2) from which the MS/MS file was obtained.^[54,61]

NMR spectroscopy: NMR spectra were recorded on a Bruker AVANCE III 600 spectrometer operating at a proton frequency of 600.05 MHz and a ¹³C frequency of 150.88 MHz. Chemical shifts (δ) are given in ppm and were referenced to the solvent signals of d₆-DMSO (¹H 2.50 and ¹³C 39.5 ppm). Measurements were done in the NMR department of the Justus-Liebig-University Giessen.

Marfey's analysis: Stereochemistry of the proteinogenic amino acids of **1** was determined by derivatization using Marfey's reagent.^[62] The stock solutions of NaHCO₃ (1 M in H₂O), amino acid standards (50 mM in H₂O), and 1-fluoro-2-4-dinitrophenyl-5-L-valine amide (D-FDVA, Sigma-Aldrich, St. Louis, MO, United States) (70 mM in acetone) were prepared. Commercially available standards (all Sigma) were derivatized using molar ratios of amino acid to D-FDVA and NaHCO₃ (1:1.4:8). To end the reaction after stirring at 40 °C for 3 h, 1 M HCl was added to obtain a final concentration of 170 mM. Total hydrolysis of **1** was done by dissolving 250 μ g in 6 M DCL in D₂O and stirring for 8 h at 160 °C. Subsequently, samples were evaporated to dryness and dissolved in DMSO to obtain a final concentration of 50 mM. All D- and L-amino acids were measured separately using C18 UHPLC-MS with the standard gradient described in the isolation section.

Bioassays: FE011 was screened against a panel of pathogenic microbes as previously described.^[59] Briefly,^[59] cell suspensions of the test strains were prepared from pre-cultures and adjusted to a concentration of 1×10^5 cells/mL before the assay. A dilution series of izoniazid or gentamicin was used as the positive control, and untreated cell suspensions were used as negative controls. End optical density readings after 24 h (*E. coli* ATCC 35218, *S. aureus* ATCC 33592 and *B. subtilis* DSM 10) or 48 h (*M. smegmatis* ATCC 607, *A. flavus* ATCC 91 and *C. albicans*) were determined using a LUMIstar Omega (BMG Labtech, Ortenberg, Germany) or ATP was quantified using BacTiter-Glo (Promega, Madison, WI, USA) according to the manufacturers' protocols. Phytotoxicity was evaluated by sterilizing *B. rapa* subsp. *rapa* seeds in 30% bleach solution and placing them in disposable culture tubes (Thermo Fisher Scientific) containing 0.32% Schenk and Hildebrandt Basal Salt Mixture (Sigma-Aldrich), solidified with 0.25% gellan gum (Sigma-Aldrich) and allowing the plants to grow at 20 °C and 40% relative humidity, with a 16-h photoperiod. Test compounds at 10, 5 and 1 μ M were applied to the plants 7 days after seeding. Phytotoxicity was confirmed if > 50% of the plant tissue was affected. Viridiol (Cayman Chemicals, Ann Harbor, MI, USA) was used as the positive control. Nematocidal activity was assessed against the model organism *Caenorhabditis elegans* N2. *C. elegans* was kept on NGM Agar plates with *E. coli* OP50 as food source.^[63] After 4 days, worms were collected in M9 buffer. Alkaline hypochlor-

ite solution (5 M NaOH + 5% NaClO 1:2) was used to isolate the worm eggs. After several washing steps (M9-buffer), the eggs were incubated overnight in NGM medium on a rotator. After incubation the tube contained solely hatched L1/L2 larvae. This synchronized worm culture was diluted to 100 worms/mL. Before the assay, the worms were supplemented with 5 μ g/mL cholesterol, 25 μ g/mL carbenicillin and *E. coli* OP50 (0.5% v/v). The solution was distributed into 96-well microtiter plates (100 μ L assay volume). FE011 was tested in an eight point dilution series (64 - 0.5 μ g/mL) in triplicate. A dilution series of Ivermectin (40–0.3 ng/mL; Sigma Aldrich) was used as positive control. A compound concentration was considered 'active' if > 85 worms were dead. The assay was incubated for 48 h at 23 \pm 3 °C. The live-dead ratio was assessed by stereo microscopy. Ivermectin showed activity at 10 ng/mL. FE011, and Ionomycin (Cayman Chemicals, Ann Arbor, MI, USA) were dissolved in DMSO to get 10 mM stock solutions. Madin-Darby canine kidney (MDCK II) cells were kindly provided by Prof. Dr. Friebertshäuser (University of Marburg). Cytotoxicity was assessed as described before.^[64] In brief, MDCK II cells were seeded in cell-culture treated 96-well microtiter plates. After reaching a confluence of 90%, cells were treated with FE011 and Ionomycin (100 μ M per well) and with the DMSO control. The plate was incubated at 37 °C and 5% CO₂ for 24 h. The cell viability was assessed by measuring the ATP content using the CellTiter-Glo Luminescent Cell Viability assay (Promega GmbH, Walldorf, Germany) according to the manufacturer's protocol. Luminescence was measured using a black 96-well plate (Greiner Bio-One GmbH, Frickenhausen, Germany) in a Synergy H4 microplate reader (Biotek [now Agilent], Bad Friedrichshall, Germany). Relative light units (RLU) were normalized to the DMSO control and set to 100%. Measurements were done with three replicates and the standard deviations were calculated using Graphpad Prism 9.1.2 (226) (GraphPad Software, LLC, San Diego, CA, USA).

Acknowledgements

This work was funded by the Hessian State Ministry of Higher Education, Research and the Arts (HMWK) via the state initiative for the development of scientific and economic excellence (LOEWE Center for Insect Biotechnology and Bioresources). Sanofi-Aventis Deutschland GmbH and Evotec International GmbH financially supported this work in the framework of the Sanofi-Fraunhofer Natural Products Center and its follow up, the Fraunhofer-Evotec Natural Products Center of Excellence. The authors thank Pascal Geisler, Franziska Warnke, Jennifer Kuhn, Nadine Zucchetto, Hamid Keyvani Hafshejani, Christine Wehr, Judith Haerter, Mona Abdullahi, Kirsten Susann Bommersheim, and Christoph Hartwig (all Fraunhofer) and Yvonne de Laval (BAM) for technical support, Prof. Dr. Rudy Plarre and Prof. Dr. Dino P. McMahon (both BAM), Prof. Dr. Thomas Degenkolb, Prof. Dr. Hans Brückner (both JLU) for valuable discussions, and Dr. Heike Hausmann (JLU) for NMR support and the NMR department of the Justus-Liebig-University Giessen for technical assistance. The authors thank Prof. Dr. Eva Friebertshäuser (University of Marburg) for kindly providing MDCK II cells. All authors read and agreed on the final version of the manuscript. Open Access funding enabled and organized by Projekt DEAL.

Conflict of Interest

L. Toti, M. Kurz and P. E. Hammann are or have been Sanofi employees and may hold shares and/or stock options in the company. P. E. Hammann and J. Glaeser are or have been employed by Evotec International GmbH.

Data Availability Statement

The data that support the findings of this study are openly available in NCBI BioProject (PRJNA) at <https://www.ncbi.nlm.nih.gov/bioproject/PRJNA788263>, reference number 788263.

Keywords: *Coptotermes testaceus* · fungal pentapeptides · insect mycobiome · metabolomics · trichoderma

- [1] E. Mevers, T. Chouvenc, N.-Y. Su, J. Clardy, *J. Chem. Ecol.* **2017**, *43*, 1078–1085.
- [2] T. Větrovský, P. Soukup, P. Stiblík, K. Votýpková, A. Chakraborty, I. O. Larrañaga, D. Sillam-Dussès, N. Lo, T. Bourguignon, P. Baldrian, et al., *Fungal Ecol.* **2020**, *48*, 100991.
- [3] T. Chouvenc, P. Bardunias, C. A. Efstathion, S. Chakraborty, M. L. Elliott, R. Giblin-Davis, N.-Y. Su, *Ann. Entomol. Soc. Am.* **2013**, *106*, 771–778.
- [4] T. Chouvenc, C. A. Efstathion, M. L. Elliott, N.-Y. Su, *Proc. Biol. Sci.* **2013**, *280*, 20131885.
- [5] T. Chouvenc, N.-Y. Su, A. Robert, *J. Invertebr. Pathol.* **2009**, *101*, 130–136.
- [6] a) I. Stefanini, *Yeast* **2018**, *35*, 315–330; b) D. Zhang, A. R. Lax, B. Henrissat, P. Coutinho, N. Katiya, W. C. Nierman, N. Fedorova, *Insect Mol. Biol.* **2012**, *21*, 235–245.
- [7] C. Wen, H. Xiong, J. Wen, X. Wen, C. Wang, *Front. Microbiol.* **2020**, *11*, 653.
- [8] V. Gouli, S. Gouli, J. A. P. Marcelino, M. Skinner, B. L. Parker, *Insects* **2013**, *4*, 631–645.
- [9] J. D. Rogers, Y.-M. Ju, J. Lehmann, *Mycologia* **2005**, *97*, 914–923.
- [10] M.-F. Li, G.-H. Li, K.-Q. Zhang, *Metabolites* **2019**, *9*, 58.
- [11] Z. Liu, Y. Sun, M. Tang, P. Sun, A. Wang, Y. Hao, Y. Wang, Y. Pei, *J. Nat. Prod.* **2020**, *83*, 3635–3641.
- [12] A. Iida, M. Sanekata, S. Wada, T. Fujita, H. Tanaka, A. Enoki, G. Fuse, M. Kanai, K. Asami, *Chem. Pharm. Bull.* **1995**, *43*, 392–397.
- [13] S. Wada, A. Iida, N. Akimoto, M. Kanai, N. Toyama, T. Fujita, *Chem. Pharm. Bull.* **1995**, *43*, 910–915.
- [14] T. Degenkolb, R. Dieckmann, K. F. Nielsen, T. Gräfenhan, C. Theis, D. Zafari, P. Chaverri, A. Ismael, H. Brückner, H. von Döhren, et al., *Mycol. Prog.* **2008**, *7*, 177–219.
- [15] H. A. Contreras-Cornejo, L. Macías-Rodríguez, E. del-Val, J. Larsen in *Reference Series in Phytochemistry* (Eds.: J.-M. Mérillon, K. G. Ramawat), Springer, Cham, **2020**.
- [16] J. F. d. S. Daniel, E. R. Filho, *Nat. Prod. Rep.* **2007**, *24*, 1128–1141.
- [17] X. Niu, N. Thaochan, Q. Hu, *J. Fungi* **2020**, *6*, 61.
- [18] M. Oberpaul, C. M. Zunkeller, T. Culver, M. Spohn, S. Mihajlovic, B. Leis, S. P. Glaeser, R. Plarre, D. P. McMahon, P. Hammann, et al., *Front. Microbiol.* **2020**, *11*, 597628.
- [19] a) B. J. Enagbonma, C. F. Ajilogba, O. O. Babalola, *Arch. Microbiol.* **2020**, *202*, 2697–2709; b) Q.-L. Chen, H.-W. Hu, Z.-Z. Yan, C.-Y. Li, B.-A. T. Nguyen, A.-Q. Sun, Y.-G. Zhu, J.-Z. He, *Soil Biol. Biochem.* **2021**, *152*, 108073.
- [20] K. R. Clarke, *Austral. Ecol.* **1993**, *18*, 117–143.
- [21] A. A. Visser, V. I. D. Ros, Z. W. de Beer, A. J. M. Debets, E. Hartog, T. W. Kuyper, T. Laessøe, B. Slippers, D. K. Aanen, *Mol. Ecol.* **2009**, *18*, 553–567.
- [22] K. Becker, M. Stadler, *J. Antibiot.* **2021**, *74*, 1–23.
- [23] G. T. Kirker, T. L. Wagner, S. V. Diehl, *Int. Biodeterior. Biodegrad.* **2012**, *72*, 18–25.
- [24] C. Beemelmans, H. Guo, M. Rischer, M. Poulsen, *Beilstein J. Org. Chem.* **2016**, *12*, 314–327.
- [25] A. P. M. Duarte, D. Attili-Angelis, N. C. Baron, L. C. Forti, F. C. Pagnocca, *Antonie van Leeuwenhoek* **2014**, *106*, 465–473.
- [26] B. J. F. d. S. Lima, M. F. Voidaleski, R. R. Gomes, G. Fornari, J. M. B. Soares, A. Bombassaro, G. X. Schneider, B. S. Da Soley, C. M. P. E. S. de Azevedo, C. Menezes, et al., *Fungal Biol.* **2020**, *124*, 194–204.
- [27] J. Kaur, R. Kaur, R. Datta, S. Kaur, A. Kaur, *J. Appl. Microbiol.* **2018**, *125*, 1455–1465.
- [28] G. Zimmermann, *Biol. Control* **2008**, *18*, 865–901.
- [29] C. A. Dunlap, M. A. Jackson, M. S. Wright, *Biocontrol. Sci. Technol.* **2007**, *17*, 513–523.
- [30] a) M. A. Jackson, S. Cliquet, L. B. Iten, *Biocontrol. Sci. Technol.* **2003**, *13*, 23–33; b) M. S. Wright, W. J. Connick, Jr, M. A. Jackson (The United States of America as represented by The Secretary of Agriculture), WO2003043417 A3, **2003**; c) S. Wraight, R. Carruthers, S. Jaronski, C. Bradley, C. Garza, S. Galaini-Wraight, *Biol. Control* **2000**, *17*, 203–217.
- [31] C. C. Staats, A. Junges, R. L. M. Guedes, C. E. Thompson, G. L. de Moraes, J. T. Boldo, L. G. P. de Almeida, F. C. Andreis, A. L. Gerber, N. Sbaraini, et al., *BMC Genomics* **2014**, *15*, 822.
- [32] M. del C. H. Rodríguez, H. C. Evans, L. M. de Abreu, D. M. de Macedo, M. K. Ndacnou, K. B. Bekele, R. W. Barreto, *Sci. Rep.* **2021**, *11*, 5671.
- [33] a) L.-H. Chen, Y.-Q. Cui, X.-M. Yang, D.-K. Zhao, Q.-R. Shen, *Australas. Plant Pathol.* **2012**, *41*, 239–245; b) R. A. A. Khan, S. Najeeb, S. Hussain, B. Xie, Y. Li, *Microorganisms* **2020**, *8*, 817.
- [34] P. K. Mukherjee, J. F. Hurley, J. T. Taylor, L. Puckhaber, S. Lehner, I. Druzhinina, R. Schumacher, C. M. Kenerley, *Biochem. Biophys. Res. Commun.* **2018**, *505*, 606–611.
- [35] J. S. Moffatt, J. D. Bu'Lock, T. H. Yuen, *J. Chem. Soc. D* **1969**, 839a–839a.
- [36] Q. Huang, Y. Tezuka, T. Kikuchi, Y. Momose, *Eur. J. Pharmacol.* **1994**, *271*, R5–R6.
- [37] W.-L. Shi, X.-L. Chen, L.-X. Wang, Z.-T. Gong, S. Li, C.-L. Li, B.-B. Xie, W. Zhang, M. Shi, C. Li, et al., *J. Exp. Bot.* **2016**, *67*, 2191–2205.
- [38] P. F. Andersson, S. B. K. Johansson, J. Stenlid, A. Broberg, *For. Pathol.* **2010**, *40*, 43–46.
- [39] E. T. Reese, *Biotechnol. Bioeng. Symp.* **1976**, 9–20.
- [40] H. Laatsch, *AntiBase: The Natural Compound Identifier*, Wiley-VCH, Weinheim, **2017**.
- [41] M. C. Pedras, L. I. Zaharia, D. E. Ward, *Phytochemistry* **2002**, *59*, 579–596.
- [42] K. S. Sree, V. Padmaja, Y. L. N. Murthy, *Pest Manage. Sci.* **2008**, *64*, 119–125.
- [43] C. Dumas, P. Robert, M. Pais, A. Vey, J.-M. Quiot, *Comp. Biochem. Physiol. Part C* **1994**, *108*, 195–203.
- [44] B. Junker, A. Walker, N. Connors, A. Seeley, P. Masurekar, M. Hesse, *Biotechnol. Bioeng.* **2006**, *95*, 919–937.
- [45] E. Matabaro, H. Kaspar, P. Dahlin, D. L. V. Bader, C. E. Murar, F. Staubli, C. M. Field, J. W. Bode, M. Künzler, *Sci. Rep.* **2021**, *11*, 3541.
- [46] J. Chatterjee, C. Gilon, A. Hoffman, H. Kessler, *Acc. Chem. Res.* **2008**, *41*, 1331–1342.
- [47] J. Chatterjee, F. Rechenmacher, H. Kessler, *Angew. Chem. Int. Ed.* **2013**, *52*, 254–269; *Angew. Chem.* **2013**, *125*, 268–283.
- [48] A. T. Bockus, J. A. Schwochert, C. R. Pye, C. E. Townsend, V. Sok, M. A. Bednarek, R. S. Lokey, *J. Med. Chem.* **2015**, *58*, 7409–7418.
- [49] A. K. Mukherjee, A. Sampath Kumar, S. Kranthi, P. K. Mukherjee, *3 Biotech* **2014**, *4*, 275–281.
- [50] R. H. Scheffrahn, T. F. Carrijo, J. Křeček, N.-Y. Su, A. L. Szalanski, J. W. Austin, J. A. Chase, J. R. Mangold, *Arthropod Syst. Phylogeny* **2015**, *73*, 333–348.
- [51] H. S. Gweon, A. Oliver, J. Taylor, T. Booth, M. Gibbs, D. S. Read, R. I. Griffiths, K. Schonrogge, *Methods Ecol. Evol.* **2015**, *6*, 973–980.
- [52] V. Robert, D. Vu, A. B. H. Amor, N. van de Wiele, C. Brouwer, B. Jabas, S. Szoke, A. Dridi, M. Triki, S. Ben Daoud, et al., *IMA Fungus* **2013**, *4*, 371–379.
- [53] Ø. Hammer, D. A. T. Harper, P. D. Ryan, *Palaeontol. Electron.* **2001**, *1*, 1–9.
- [54] M. Marner, M. A. Patras, M. Kurz, F. Zubeil, F. Förster, S. Schuler, A. Bauer, P. Hammann, A. Vilcinskis, T. F. Schäberle, et al., *J. Nat. Prod.* **2020**, *83*, 2607–2617.
- [55] K. Panzer, P. Yilmaz, M. Weiß, L. Reich, M. Richter, J. Wiese, R. Schmaljohann, A. Labes, J. F. Imhoff, F. O. Glöckner, et al., *PLoS One* **2015**, *10*, e0134377.
- [56] M. C. Chambers, B. Maclean, R. Burke, D. Amodei, D. L. Ruderman, S. Neumann, L. Gatto, B. Fischer, B. Pratt, J. Egertson, et al., *Nat. Biotechnol.* **2012**, *30*, 918–920.
- [57] J. Y. Yang, L. M. Sanchez, C. M. Rath, X. Liu, P. D. Boudreau, N. Bruns, E. Glukhov, A. Wodtke, R. de Felicio, A. Fenner et al., *J. Nat. Prod.* **2013**, *76*, 1686–1699.
- [58] F. Allen, R. Greiner, D. Wishart, *Metabolomics* **2015**, *11*, 98–110.

- [59] M. Oberpaul, S. Brinkmann, M. Marner, S. Mihajlovic, B. Leis, M. A. Patras, C. Hartwig, A. Vilcinskas, P. E. Hammann, T. F. Schäberle et al., *Microb. Biotechnol.* **2021**, *15*, 415–430.
- [60] a) N. A. Reisdorph, S. Walmsley, R. Reisdorph, *Metabolites* **2019**, *10*, 8;
b) L. W. Sumner, A. Amberg, D. Barrett, M. H. Beale, R. Beger, C. A. Daykin, T. W.-M. Fan, O. Fiehn, R. Goodacre, J. L. Griffin et al., *Metabolomics* **2007**, *3*, 211–221.
- [61] P. Shannon, A. Markiel, O. Ozier, N. S. Baliga, J. T. Wang, D. Ramage, N. Amin, B. Schwikowski, T. Ideker, *Genome Res.* **2003**, *13*, 2498–2504.
- [62] R. Bhushan, H. Brückner, *Amino Acids* **2004**, *27*, 231–247.
- [63] T. Stiernagle, *Maintenance of C. elegans* (February 11, **2006**). *WormBook* (Ed.: The *C. elegans* Research Community), WormBook, Available online: <http://www.wormbook.org> (accessed on 25 January 2022).
- [64] J. Krämer, T. Lüddecke, M. Marner, E. Maiworm, J. Eichberg, K. Hards, T. F. Schäberle, A. Vilcinskas, R. Predel, *Toxin Rev.* **2022**, *14*, 58.

Manuscript received: December 22, 2021
Revised manuscript received: March 16, 2022
Accepted manuscript online: March 17, 2022
Version of record online: April 1, 2022